# Perfect absorption in a monolayer graphene at the near-infrared using a compound waveguide grating by robust critical coupling

**Jinhua Hu (胡劲华)[1], Jia Fu (付 佳)[1], Xiuhong Liu (刘秀红)[2,*], Danping Ren (任丹萍)[1], Jijun Zhao (赵继军)[1], and Yongqing Huang (黄永清)[3,**]**

[1]*School of Information & Electrical Engineering, Hebei University of Engineering, Handan 056038, China*
[2]*School of Mathematics & Physics, Hebei University of Engineering, Handan 056038, China*
[3]*State Key Laboratory of Information Photonics and Optical Communications, Beijing University of Posts and Telecommunications, Beijing 100876, China*
**Corresponding author: liuxiuhong@hebeu.edu.cn; **corresponding author: yqhuang@bupt.edu.cn*
Received August 13, 2018; accepted November 12, 2018; posted online December 20, 2018

We present a perfect graphene absorber with a compound waveguide grating at the near-infrared. The analytical approach is mainly based on the coupled leaky mode theory, which turns the design of the absorber to finding out the required leaky modes supported by the grating structure. Perfect absorption occurs only when the radiative loss of the leaky mode matches the intrinsic absorption loss, which is also named the critical coupling condition. Furthermore, we also demonstrate that the critical coupling of the system can be robustly controlled, and the perfect absorption wavelength can be easily tuned by adjusting the parameters of the compound waveguide grating.

*OCIS codes: 050.6624, 140.4780, 230.7408.*
*doi: 10.3788/COL201917.010501.*

Graphene has attracted research interest as a promising platform in optoelectronics because of its exceptional electronic and optical properties. Many graphene-based devices, such as photodetectors[1], modulators[2], sensors[3], nanoantennas[4], tunable Bragg reflectors[5], and absorbers[6–8] have been intensively studied in recent years. However, there are two inherent limitations in monolayer graphene, which hinder its further application in active devices. The first one is that the absorption of graphene is only 2.3% for normal incident light in the infrared wavelength region[9]. The second one is that monolayer graphene has no spectral selectivity in both the visible and infrared spectral ranges. At the same time, it is very difficult to enhance the absorption efficiency of undoped and unpatterned monolayer graphene across visible to near-infrared wavelengths ($\lambda < 2$ μm) by exciting graphene plasmons (GPs). Therefore, resonant dielectric structures, such as photonic crystal slabs[10] and resonant dielectric gratings[11–13], have become very popular in enhancing light absorption of graphene in the near-infrared regions due to their easy fabrication and low transmission loss. Total absorption in a graphene monolayer at near-infrared has been recently proposed via concepts of critical coupling and guided resonance[14,15]. Meanwhile, the physical mechanism of critical coupling that is giving rise to total absorption can be explained by the temporal coupled-mode theory (TCMT)[16,17]. In our previous study, we achieve total light absorption at the near-infrared wavelength with graphene strips by using critical coupling, which is associated with guided resonance of subwavelength multilayer grating structures[18]. However, the total absorption is sensitive to the change of the incident angle. In a recent study, tunable enhanced absorbers with spectrum selectivity have been presented using the compound grating structure in Ref. [12]. However, the total absorption was also difficult to be remained with varying structural parameters (i.e., gap of the compound grating structure). Physically, the total absorption of a graphene-based absorber can be achieved near the condition of critical coupling, at which the external leakage rate is equal to the intrinsic loss rate. Thus, it is quite necessary to find a structure that can still realize critical coupling even when a small variation of the structure parameters is introduced. That also means that the critical coupling condition can be robustly controlled. Besides, most of the structures are designed by rigorous coupled wave analysis (RCWA)[19–21] and finite-difference time-domain (FDTD)[22], which often rely on heavy computation and a lack of an intuitive relationship between critical coupling and structural parameters of the resonant structure.

In this work, we theoretically investigate optical absorption in monolayer graphene, which is covered on the top of a compound waveguide grating (CWG)[23,24], at normal incidence using critical coupling based on the coupled leaky mode theory (CLMT) in the telecommunication wavelength range[25–27]. The CLMT model, which is an intuitive theoretical model, considers optical absorption as optical coupling between the incident light wave and leaky modes of resonant structures. Using this model, the critical coupling of the resonant system with total absorption can be evaluated with a straightforward relationship between eigenvalues of the leaky modes and physical features.

 

Here, the critical coupling of the resonant system can be robustly controlled even with the variations of structural parameters in the CWG structure, such as grating thickness, grating period, and the gap of the compound grating ridges. These results are valuable in guiding the design of perfect active devices, including photodetectors and modulators.

Figure 1 shows a schematic of the proposed graphene-based absorber and an $x$–$z$ cross-section plane of the device. The presented structure consists of a monolayer graphene, a CWG, and a dielectric Bragg reflector (DBR) of 4.5 pair $Si/SiO_2$ layers. Using the DBR as a back-reflection mirror, the transmission of the TE-polarized light can be prevented at normal incidence. The CWG is composed of a silicon slab waveguide layer and a silicon grating layer with two different grating ridges in a period, respectively. The structure is finitely periodic in the $x$ direction and uniform along the $y$ direction. The key parameters of the device are defined as follows: the width of the gap between the two grating ridges is $G$. The widths of two grating ridges are denoted as $W_1$ and $W_2$, respectively. The grating period of the CWG is $P$, and the thicknesses of the grating layer and slab waveguide layer are described as $t_g$ and $t_b$, respectively.

To achieve the critical coupling of the graphene-based absorber, the absorber can be viewed as a single-mode lossless resonator. Here, the scattering loss is negligible. Thus, the absorption efficiency $A$ can be expressed as the following equation by using the TCMT model[14]:

$$A(\omega) = \frac{4\delta\gamma}{(\omega-\omega_0)^2 + (\delta+\gamma)^2}, \tag{1}$$

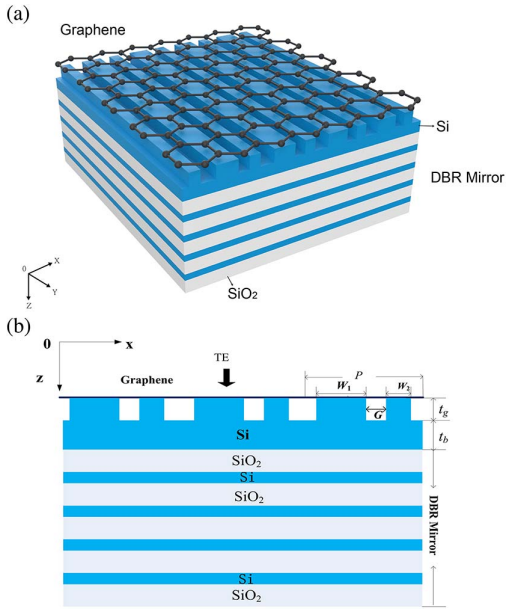


Fig. 1. Schematic of the graphene-based absorber. (a) Monolayer graphene covered on the top of the CWG with a DBR mirror. (b) Cross-section of the absorber for TE-polarized light at normal incidence.

where the central resonant frequency is $\omega_0$, the external leakage rate is $\gamma$, and intrinsic loss rate is $\delta$. We calculate the optical spectra of the multilayer structure covered with and without graphene using the RCWA method, respectively. The spectral linewidth of the resonance of the multilayer structure with graphene gives us $\delta+\gamma$, while that of the resonance of the structure without graphene gives us the external leakage rate $\gamma$. In addition, the central resonant frequency $\omega_0$ of the resonant graphene-based absorber can be obtained. According to Eq. (1), total absorption of the resonant system can be achieved at the resonance when the external leakage rate is equal to its intrinsic loss rate.

In the remainder of this work, we study the absorber with the following parameters. The graphene monolayer has the thickness of $t_0 = 0.34$ nm, and its refractive index can be expressed as $n_{\mathrm{gra}} = 3 + j5.446\lambda/3$[28]. The refractive indices of Si and $SiO_2$ are chosen as $n_{\mathrm{Si}} = 3.477$ and $n_{\mathrm{SiO_2}} = 1.45$ for the operation wavelength of 1550 nm, respectively. The thicknesses of the silica and silicon grating layers are set to be $\lambda_0/4n_{\mathrm{Si}} = 112$ nm and $3\lambda_0/4n_{\mathrm{SiO_2}} = 802$ nm, respectively. Therefore, the effective refractive index of the grating layer covered with monolayer graphene can be calculated by

$$n_{\mathrm{eff}} = \frac{n_{\mathrm{Si}}t_g + n_{\mathrm{Si}}t_b + n_{\mathrm{gra}}t_0}{t_g + t_b + t_0}. \tag{2}$$

According to Eq. (2), the effective refractive index can be estimated as $n_{\mathrm{eff}} = n_{\mathrm{real}} + in_{\mathrm{imag}}$, where $n_{\mathrm{real}}$ and $n_{\mathrm{imag}}$ are the real and imaginary parts of the refractive index of the material, respectively.

In order to intuitively understand the physical mechanism of the presented absorber, we focus on investigating the resonant light absorption in this structure based on the CLMT model. The eigenvalue of the leaky mode in the CWG with a DBR mirror can be calculated for such a resonant structure using the finite-element method (FEM)[29,30]. In order to fit the resonant wavelength from RCWA simulation, a small correction is applied to the real part of the eigenvalue $N$, which is expressed by $N = N_{\mathrm{real}} - iN_{\mathrm{imag}}$. Intrinsic absorption loss of the materials and the radiative loss of the leaky mode are then described as $n_{\mathrm{imag}}/n_{\mathrm{real}}$ and $N_{\mathrm{imag}}/N_{\mathrm{real}}$, respectively. Therefore, the absorption efficiency $A$ is described by means of the corrected eigenvalue of the leaky mode as follows[31]:

$$A(\lambda) = \frac{4N_{\mathrm{imag}}/N_{\mathrm{real}} \times n_{\mathrm{imag}}/n_{\mathrm{real}}}{\left(\frac{n_\lambda \lambda}{n_0\lambda_0} - 1\right)^2 + (N_{\mathrm{imag}}/N_{\mathrm{real}} + n_{\mathrm{imag}}/n_{\mathrm{real}})^2}, \tag{3}$$

where $n_\lambda$ and $n_0$ are the refractive index of the materials at $\lambda$ and $\lambda_0$, respectively, and $\lambda_0$ is the resonant wavelength. According to Eq. (3), total absorption of the structure can be achieved by critical coupling at the resonance wavelength with $N_{\mathrm{imag}}/N_{\mathrm{real}}$ approaching $n_{\mathrm{imag}}/n_{\mathrm{real}}$.

As an example, the structural parameters of the absorber are chosen as follows: $P = 710$ nm, $W_1 = 200$ nm, $W_2 = 150$ nm, $G = 25$ nm, $t_g = 220$ nm, and $t_b = 270$ nm. Here, the input light is assumed as TE polarization under normal incidence. We calculate the absorption spectrum of the structure using the RCWA method and obtain its parameters, such as $\omega_0$, $\gamma$, and $\delta$. We further compute the eigenvalues of the leaky mode of the proposed structure under TE polarization using the FEM. After we make a small correction using the resonant wavelength from RCWA simulated results, the eigenvalue of the leaky mode is expressed as a complex normalized parameter $N = 6.9029–0.0034i$.

According to Eq. (2), the effective refractive index can be estimated as $n_{\text{eff}} = 3.4774 + 0.002i$ at the wavelength of 1550 nm, which means the absorption loss $n_{\text{imag}}/n_{\text{real}} = 5.75 \times 10^{-4}$. Using these parameters, we calculated the theoretical absorption spectrum using Eqs. (1) and (3), respectively. We compared the theoretical results obtained from the CLMT model with the results from the RCWA and TCMT methods, respectively. As a result, the CLMT calculated results for the absorber is reasonably consistent with the other two methods. Therefore, the resonance of the absorber can be excited under the critical coupling condition at a resonant wavelength of 1550.8 nm in Fig. 2.

In order to further verify the efficient absorption of the resonator at normal incidence under TE polarization, we plot the electric (E)-field distributions at wavelengths of 1550.8 nm (on-resonant) and 1540 nm (off-resonant), as shown in Figs. 3(a) and 3(b), respectively. We find that the E-field intensity distribution around the graphene monolayer in this structure can be significantly enhanced for the on-resonant wavelength in Fig. 3(a). Obviously, the resonance of the absorber is excited at the on-resonant wavelength. In contrast, the resonant cavity is not excited for the non-resonant wavelength, as is shown in Fig. 3(b). It means that the critical coupling can be obtained at a resonant wavelength by means of the optical coupling between the incident light and its leaky resonance mode.

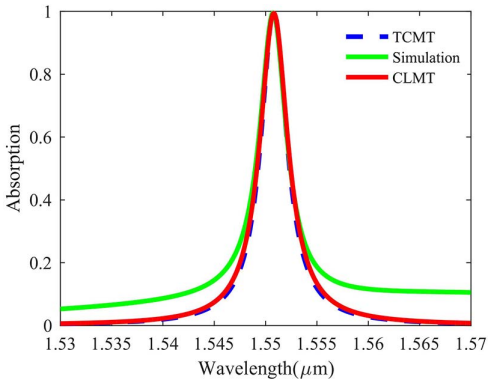


Fig. 2. RCWA simulation result and theoretically calculated result of the absorption spectrum for TE polarization light at normal incidence.

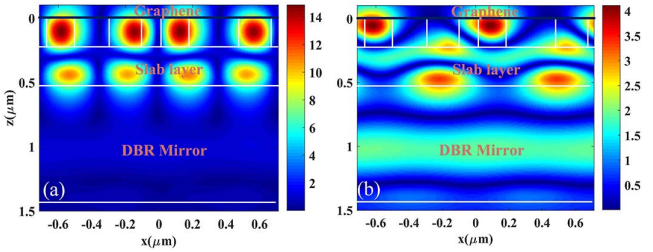


Fig. 3. Electric field amplitude distributions of the graphene-based absorber for TE polarization under normal incidence at the (a) on-resonant wavelength of 1550.8 nm and (b) off-resonant wavelength of 1540 nm.

We further compute the eigenvalues of the TE eigenmodes of the proposed structure with different gap $G$ using FEM. Comparing the resonant wavelength from the RCWA simulated results, the eigenvalues $N$ are listed in Table 1. We can see that the resonant frequency obviously decreases with the increase of $G$. In other words, the resonant wavelength exhibits a red shift as $G$ increases. As shown in Table 1, the radiative loss of the leaky mode of each structure increases with the increase of $G$. The spectrum widths will be controlled by changing the gap $G$.

Figure 4 shows the absorption spectrum of the proposed absorber with respect to wavelength and gap $G$ for TE-polarized light using RCWA. As shown in the figure, a good absorption still remains in spite of an obvious change of the gap $G$. Meanwhile, the resonant wavelength significantly increases with an increasing gap $G$, whereas the

**Table 1.** Eigenvalues of TE Eigenmodes Corresponding to Different Gap $G$

| $G$ (nm) | Eigenvalue $N$ | $N_{\text{imag}}/N_{\text{real}}$ |
|---|---|---|
| 25 | 6.9029-0.0034$i$ | $4.9254 \times 10^{-4}$ |
| 30 | 6.8774-0.0044$i$ | $6.3977 \times 10^{-4}$ |
| 35 | 6.8530-0.0050$i$ | $7.2702 \times 10^{-4}$ |

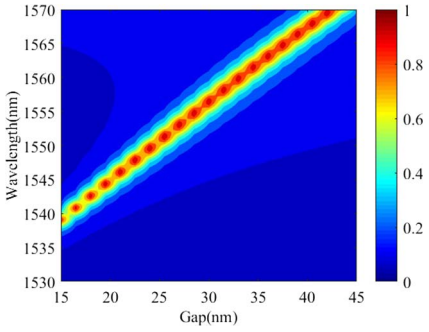


Fig. 4. Absorption spectra in the structure as a function of wavelength and gap $G$ using RCWA. The remaining parameters are set to $P = 710$ nm, $W_1 = 200$ nm, $W_2 = 150$ nm, $t_g = 220$ nm, and $t_b = 270$ nm.

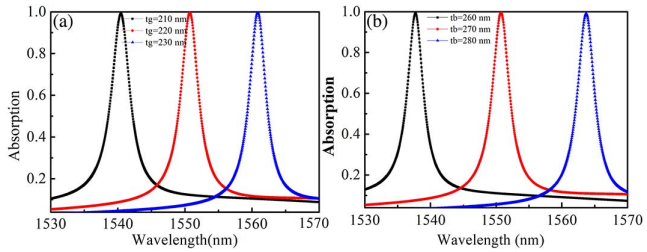


Fig. 5. Absorption spectra of the structure as a function of wavelength for different grating thickness $t_g$ and slab thickness $t_b$. $P = 710$ nm, $W_1 = 200$ nm, $W_2 = 150$ nm, and $G = 25$ nm, (a) $t_b = 270$ nm, (b) $t_g = 220$ nm.

linewidth of the absorption spectrum increases with the increase of the gap $G$. In other words, the critical coupling is fairly robust for such a resonant system with the changing of $G$. Thus, the proposed compound grating structure plays an important role in controlling the absorption response of monolayer graphene at the near-infrared.

Figure 5 shows the absorption spectrum of the structure with respect to different grating thickness $t_g$ and slab thickness $t_b$ for TE-polarized light calculated with the CLMT model. The resonant absorption peak can be tuned by changing the grating thickness $t_g$ and the silicon slab thickness $t_b$ while maintaining $G$ and $P$. As the grating thickness increases, the resonant wavelength shows red shifts, as shown in Fig. 5(a). Similarly, increasing the slab thickness pushes the resonant wavelength to a long wavelength, as illustrated in Fig. 5(b). We can see that total absorption is maintained in spite of significant changes of the resonant wavelengths while simultaneously and independently varying grating thickness and silicon slab thickness. It means that the critical coupling of the resonant system is fairly robust. Meanwhile, the linewidth of the absorption spectrum of the absorber is significantly determined by the gap $G$. This indicates that radiative loss of the leaky resonance can be sufficiently controlled by the gap of the CWG structure.

In summary, we have presented a graphene-based perfect absorber based on a CWG with a back reflector. The optical absorption of the graphene-based structure was studied by the CLMT. Critical coupling of the absorber can be robustly controlled in spite of the change of its structure parameters. The proposed absorber has potential applications in developing high-performance optical devices, such as photodetectors and modulators.

This work is supported in part by the National Key Research and Development Program of China (No. 2018YFF0301004), the Scientific Research Projects of the Department of Education of Hebei Province (No. QN2016090), the National Natural Science Foundation of Hebei Province (Nos. F2017402068, F2018402198, and A2015402035), the Research Program for Top-notch Young Talents in Higher Education Institutions of Hebei Province (No. BJ2017037), and the Research and Development Program for Science and Technology of Handan (No. 1621203037).

## References

1. X. Gan, R. J. Shiue, Y. Gao, I. Meric, T. F. Heinz, K. Shepard, J. Hone, S. Assefa, and D. Englund, Nat. Photon. **7**, 883 (2013).
2. M. Liu, X. Yin, E. Ulin-Avila, B. Geng, T. Zentgraf, L. Ju, F. Wang, and X. Zhang, Nature **474**, 64 (2011).
3. Y. Long, Y. Li, L. Shen, W. Liang, H. Deng, and H. Xu, J. Phys. D: Appl. Phys. **49**, 32LT01 (2016).
4. X. Ren, W. E. I. Sha, and W. C. H. Choy, Opt. Express **21**, 31824 (2013).
5. J. Tao, X. C. Yu, B. Hu, A. Dubrovkin, and Q. J. Wang, Opt. Lett. **39**, 271 (2014).
6. M. Grande, M. A. Vincenti, T. Stomeo, G. V. Bianco, D. de Ceglia, N. Aközbek, V. Petruzzelli, G. Bruno, M. De Vittorio, M. Scalora, and A. D'Orazio, Opt. Express **22**, 31511 (2014).
7. M. Grande, M. A. Vincenti, T. Stomeo, G. V. Bianco, D. de Ceglia, N. Aközbek, V. Petruzzelli, G. Bruno, M. De Vittorio, M. Scalora, and A. D'Orazio, Opt. Express **23**, 21032 (2015).
8. H. Meng, X. Xue, Q. Lin, G. Liu, X. Zhai, and L. Wang, Appl. Phys. Express **11**, 052002 (2018).
9. R. R. Nair, P. Blake, A. N. Grigorenko, K. S. Novoselov, T. J. Booth, T. Stauber, N. M. R. Peres, and A. K. Geim, Science **320**, 1308 (2008).
10. Y. Liu, A. Chadha, D. Zhao, J. R. Piper, Y. Jia, Y. Shuai, L. Menon, H. Yang, Z. Ma, S. Fan, F. Xia, and W. Zhou, Appl. Phys. Lett. **105**, 181105 (2014).
11. C. C. Guo, Z. H. Zhu, X. D. Yuan, W. M. Ye, K. Liu, J. F. Zhang, W. Xu, and S. Q. Qin, Adv. Opt. Mater. **4**, 1955 (2016).
12. G. Zheng, X. Zou, Y. Chen, L. Xu, and Y. Liu, Plasmonics **12**, 1177 (2017).
13. T. Sang, R. Wang, J. Li, J. Zhou, and Y. Wang, Opt. Commun. **413**, 255 (2018).
14. J. R. Piper and S. Fan, ACS Photon. **1**, 347 (2014).
15. A. Yariv, IEEE Photon. Technol. Lett. **14**, 483 (2002).
16. S. Fan, W. Suh, and J. D. Joannopoulos, J. Opt. Soc. Am. A. **20**, 569 (2003).
17. H. A. Haus, *Waves and Fields in Optoelectronics* (Prentice Hall, 1984).
18. J. H. Hu, Y. Q. Huang, X. F. Duan, Q. Wang, X. Zhang, J. Wang, and X. M. Ren, Appl. Phys. Lett. **105**, 221113 (2014).
19. M. G. Moharam, E. B. Grann, D. A. Pommet, and T. K. Gaylord, J. Opt. Soc. Am. A **12**, 1068 (1995).
20. M. G. Moharam, D. A. Pommet, E. B. Grann, and T. K. Gaylord, J. Opt. Soc. Am. A **12**, 1077 (1995).
21. L. Li, J. Opt. Soc. Am. A. **13**, 1870 (1996).
22. A. Taflove and S. C. Hagness, *Computational Electrodynamics: The Finite-Difference Time-Domain Method* (Artech House, 2005).
23. X. Cui, H. Tian, Y. Du, G. Shi, and Z. Zhou, Sci. Rep. **6**, 36066 (2016).
24. W. Liu, Y. Li, H. Jiang, Z. Lai, and H. Chen, Opt. Lett. **38**, 163 (2013).
25. Y. Yu and L. Cao, Opt. Express **20**, 13847 (2012).
26. Y. Yu and L. Cao, Opt. Express **21**, 5957 (2013).
27. L. Huang, Y. Yu, and L. Cao, Nano Lett. **13**, 3559 (2013).
28. M. Bruna and S. Borini, Appl. Phys. Lett. **94**, 031901 (2009).
29. J. Hu, X. Liu, J. Zhao, and J. Zou, Chin. Opt. Lett. **15**, 030502 (2017).
30. J. Hu, Y. Huang, X. Ren, X. Duan, Y. Li, Q. Wang, X. Zhang, and J. Wang, Chin. Phys. Lett. **31**, 064205 (2014).
31. L. Huang, G. Li, A. Gurarslan, Y. Yu, R. Kirste, W. Guo, J. Zhao, R. Collazo, Z. Sitar, N. Parsons, M. Kudenov, and L. Cao, ACS Nano **10**, 7493 (2016).